# Vitamin D Is a Regulator of Endothelial Nitric Oxide Synthase and Arterial Stiffness in Mice

Olena Andrukhova,* Svetlana Slavic,* Ute Zeitz, Sabine C. Riesen, Monika S. Heppelmann, Tamas D. Ambrisko, Mato Markovic, Wolfgang M. Kuebler, and Reinhold G. Erben

Department of Biomedical Research (O.A., S.S., U.Z., M.S.H., R.G.E.) and Department for Companion Animals and Horses (S.C.R., T.D.A., M.M.), University of Veterinary Medicine Vienna, 1210 Vienna, Austria; and Institute for Surgical Research (W.M.K.), Ludwig Maximilians University, 80539 Munich, Germany

The vitamin D hormone 1$\alpha$,25-dihydroxyvitamin $D_3$ [1,25(OH)$_2$D$_3$] is essential for the preservation of serum calcium and phosphate levels but may also be important for the regulation of cardiovascular function. Epidemiological data in humans have shown that vitamin D insufficiency is associated with hypertension, left ventricular hypertrophy, increased arterial stiffness, and endothelial dysfunction in normal subjects and in patients with chronic kidney disease and type 2 diabetes. However, the pathophysiological mechanisms underlying these associations remain largely unexplained. In this study, we aimed to decipher the mechanisms by which 1,25(OH)$_2$D$_3$ may regulate systemic vascular tone and cardiac function, using mice carrying a mutant, functionally inactive vitamin D receptor (VDR). To normalize calcium homeostasis in VDR mutant mice, we fed the mice lifelong with the so-called rescue diet enriched with calcium, phosphate, and lactose. Here, we report that VDR mutant mice are characterized by lower bioavailability of the vasodilator nitric oxide (NO) due to reduced expression of the key NO synthesizing enzyme, endothelial NO synthase, leading to endothelial dysfunction, increased arterial stiffness, increased aortic impedance, structural remodeling of the aorta, and impaired systolic and diastolic heart function at later ages, independent of changes in the renin-angiotensin system. We further demonstrate that 1,25(OH)$_2$D$_3$ is a direct transcriptional regulator of endothelial NO synthase. Our data demonstrate the importance of intact VDR signaling in the preservation of vascular function and may provide a mechanistic explanation for epidemiological data in humans showing that vitamin D insufficiency is associated with hypertension and endothelial dysfunction. (*Molecular Endocrinology* 28: 53–64, 2014)

The vitamin D hormone 1$\alpha$,25-dihydroxyvitamin $D_3$ [1,25(OH)$_2$D$_3$] is a steroid hormone essential for the control of calcium, phosphate, and bone metabolism. It acts through an intracellular receptor protein, the vitamin D receptor (VDR), which is a ligand-activated transcription factor binding to vitamin D response elements in the promoter region of target genes. The VDR is widely distributed throughout the body, and 1,25(OH)$_2$D$_3$ may have important physiological functions beyond calcium homeostasis. Epidemiological data in humans have shown that vitamin D insufficiency is associated with car-

diovascular diseases, hypertension, left ventricular (LV) hypertrophy, increased arterial stiffness, and endothelial dysfunction in normal subjects and in patients with chronic kidney disease and type 2 diabetes (1–7). Moreover, vitamin D deficiency is associated with a profoundly increased risk for preeclampsia, a disease in pregnant women characterized by hypertension and endothelial dysfunction (8). However, the pathophysiological mechanisms underlying these associations remain largely unexplained.

Earlier studies in global VDR knockout mice suggested that lack of vitamin D signaling causes hypertension and

myocardial hypertrophy through activation of the renin-angiotensin-aldosterone system (RAAS) (9). The RAAS is an important endocrine system controlling vascular tone, peripheral vascular resistance and volume homeostasis. More recently, it was reported that cardiomyocyte-specific VDR ablation also results in heart hypertrophy, independent of changes in the RAAS (10). Notably, however, the hypertrophic cardiac changes observed in the above-mentioned mouse studies cannot explain the association between vascular tone and vitamin D insufficiency in humans (11).

In the current study, we examined cardiovascular function in mice carrying a mutant, functionally inactive vitamin D receptor (VDR$^{\Delta/\Delta}$) (12). Global VDR knockout mice fed normal mouse chow develop severe secondary hyperparathyroidism due to an intestinal calcium absorption defect and subsequent hypocalcemia (12). To normalize calcium homeostasis in VDR$^{\Delta/\Delta}$ mice, we fed the mice lifelong with the so-called rescue diet enriched with calcium, phosphate, and lactose (12, 13). Here, we report that older VDR$^{\Delta/\Delta}$ mice fed with the rescue diet are characterized by increased arterial stiffness and aortic impedance through chronically lower bioavailability of the vasodilator nitric oxide (NO).

## Materials and Methods

### Animals

All animal procedures were approved by the ethics committees of the University of Veterinary Medicine Vienna (Vienna, Austria) and of the local government authorities. The mice were kept at 24°C with a 12:12-hour light/dark cycle and were allowed free access to their diet and tap water. Wild-type (WT) and homozygous VDR$^{\Delta/\Delta}$ mutant mice were bred by intercrossing heterozygous animals. All mice had been backcrossed to the C57BL/6 genetic background for more than 10 generations. Mice were genotyped from tail biopsy samples by PCR analysis of genomic DNA as described previously (12). The normal diet (Ssniff) contained 0.9% calcium, 0.7% phosphorus, and 600 IU of vitamin D/kg. The rescue diet (Ssniff) containing 2.0% calcium, 1.25% phosphorus, 20% lactose, and 600 IU of vitamin D/kg was fed starting from 16 days of age. This diet has been shown to normalize mineral homeostasis in VDR-ablated mice (12, 13). Male mice were used in the present study for all experiments. Urine was collected in metabolic cages during a 12-hour period overnight before necropsy or catheterization. At necropsy, mice were exsanguinated from the abdominal vena cava under anesthesia with ketamine/xylazine (67/7 mg/kg ip) for serum collection.

### Histology

Hearts and aortas were fixed in 4% paraformaldehyde (PFA) embedded in paraffin and sectioned at 5-$\mu$m thickness. The morphology of heart and aorta was examined after hematoxylin and eosin staining. Cardiac fibrotic tissue was visualized by Masson trichrome staining, whereas aortic elastic lamellae were stained with resorcin-fuchsin.

### Aldosterone concentration and renin activity

Serum and urinary aldosterone levels were determined by ELISA (NovaTec) according to the manufacturer's protocol. Plasma renin activity was measured by RIA (GammaCoat; DiaSorin) according to the manufacturer's protocol.

### Central arterial pressure measurements and cardiac catheterization

Central arterial pressure and cardiac hemodynamic parameters were assessed using a SPR-671NR pressure catheter (1.4 French; Millar Instruments). Mice were anesthetized with 1.5% isoflurane in oxygen. When the paw pinch reflex had disappeared, the catheter was inserted into the ascending aorta for measurement of central arterial pressure. Parameters of LV function (ie, maximum rate of the pressure rise, contractility index, end-diastolic pressure, and isovolumetric relaxation time) were measured by placing the catheter into the left ventricle. All pressure recordings were performed at the same anesthesia level. Hemodynamic measurements were recorded over 5 minutes, and traces were analyzed using LabChartPro software and a blood pressure (BP) module. After pressure measurements, all animals were euthanized.

### Measurement of aortic impedance and augmentation index

Aortic input impedance was determined from aortic BP and flow velocity signals as described previously (14). The ascending aortic flow velocity signal was recorded using a 10-MHz digital probe placed below the xiphoid process and oriented toward the left ventricular outflow tract. A computer-based real-time Doppler spectrum analyzer (DSPW; Indus Instruments) was used to acquire the Doppler signals at a sampling rate of 125 kHz along with the BP recordings. Input impedance was defined as the ratio of pressure to luminal average blood velocity (14). The aortic augmentation index was identified from the late systolic portion of the arterial pressure wave as described previously (15, 16). The augmentation index was defined as the height from the augmentation point to the systolic peak of the pressure wave divided by the pulse pressure and is expressed as a percentage.

### Elastin and collagen content

Elastin was quantified in mouse thoracic aortas (1.5–2 cm) using a method described by Wolinsky (17) with some modifications. After delipidation in acetone-diethyl ether (1:1, vol/vol), tissue was dried, and the dry weight was determined in milligrams. Cellular proteins were extracted in 0.3% SDS. The extracellular proteins, other than elastin, were solubilized by three 20-minute extractions in 3 mL of 0.1 N sodium hydroxide in a boiling water bath. The total elastin content was quantified by the dry weight of the residue and expressed as micrograms per milligram of dry weight aorta. The extracellular proteins, including collagen, present in the sodium hydroxide were evaporated to dryness and hydrolyzed in 6 N hydrochloric acid in vacuum-sealed vials for 24 hours at 110°C. The hydroxyproline content of the hydrolysate was assayed by the method of Woess-

ner (18). Collagen was quantified from hydroxyproline on the basis of the assumption that collagen contains 12.8% hydroxyproline by weight (19) and expressed as micrograms per milligram of aortic wall tissue (dry weight).

## Scanning electron microscopy

For scanning electron microscopy, the elastin residue were prepared as described above and fixed overnight with 1.5% glutaraldehyde in Hanks' balanced salt solution. After dehydration with a graded ethanol series, critical point drying, and sputter coating with palladium gold (CPD 030; Bal-Tec), samples were examined with a JEOL 5910LV scanning electron microscope.

## Nitric oxide (NO) assay

Serum and urinary NO concentrations were measured using a commercially available colorimetric assay (Cayman Chemical Company) according to the manufacturer's protocol. Before analysis, traces of hemoglobin and proteins were removed from serum samples by ultrafiltration using Amicon Ultra-4 centrifugal filters (Merck Millipore).

## Laser capture microdissection

Cryosections from thoracic aortas were prepared from snap-frozen tissues and quickly stained with HistoStain (Arcturus). The endothelial and the smooth muscle cell layers were harvested using a Veritas (Arcturus) laser capture microdissection system. Sections of total aorta were collected for reference and RNA quality control. RNA was extracted using the PicoPure RNA isolation kit (QIAGEN).

## RNA isolation and quantitative RT-PCR

Shock-frozen tissues were homogenized in TRI Reagent (Molecular Research Center), and total RNA was extracted according to the manufacturer's protocol. RNA purity and quality were determined spectrophotometrically (BioPhotometer; Eppendorf) and via a 2100 Bioanalyzer (Agilent Technologies). One microgram of RNA was used for first-strand cDNA synthesis (iScript cDNA Synthesis Kit; Bio-Rad Laboratories). Quantitative RT-PCR was performed on a Rotor-Gene 6000 (Corbett Life Science) using QuantiFast EverGreen PCR Kit (QIAGEN). A melting curve analysis was done for all assays. Primer sequences are available on request. Efficiencies were examined by standard curve. Regulation of gene expression was calculated according to Pfaffl (20). Expression of target genes was normalized to the expression of the housekeeping gene GAPDH or ornithine decarboxylase antizyme 1.

## Western blotting

Protein samples were fractionated on SDS-PAGE (50 $\mu$g/well) and transferred to a nitrocellulose membrane (Thermo Fisher Scientific). Immunoblots were incubated for 3 hours at room temperature with primary antibodies anti–endothelial nitric oxide synthase (NOS3) (Thermo Scientific) or anti-$\beta$-actin (Sigma-Aldrich). After washing, membranes were incubated with anti-rabbit horseradish peroxidase-conjugated secondary antibodies (Amersham Life Sciences). Specific signals were visualized by an ECL kit (Amersham Life Sciences).

## LacZ staining

To visualize lacZ reporter gene expression, pre-embedding X-gal staining of aortas from WT and VDR$^{\Delta/\Delta}$ mice was performed as described previously (21). In brief, the aorta or parathyroid gland used as a positive control was prefixed with 2% PFA-0.2% glutaraldehyde at pH 8.0 for 1 hour and stained overnight in X-gal staining solution at pH 8.0. After postfixation in 4% PFA, the specimens were embedded in paraffin, sectioned at 5 $\mu$m thickness, and counterstained with nuclear fast red.

## In vitro aorta organ culture

Aortic rings (0.5–1 mm) for organ culture were prepared under sterile conditions from freshly dissected thoracic aortas of male 3-month-old WT and VDR mutant mice. The tissue was preincubated in serum-free MEM medium (PAA) containing 2% penicillin/streptomycin at 37°C in a sterile incubator with a 95% air/5% $CO_2$ atmosphere for 1 hour and then treated with $10^{-8}$ M 1$\alpha$,25(OH)$_2$D$_3$ or $10^{-7}$ M 25-hydroxyvitamin D3 [25(OH)D$_3$] (both Sigma-Aldrich) or vehicle for 24 hours. The samples were then collected for mRNA isolation.
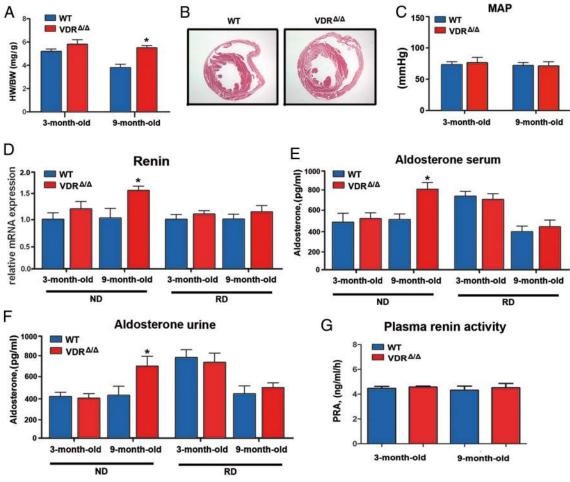
## In vitro transient transfection experiments

The pCMV6 plasmid construct containing human VDR open reading frame (RC219628; Origene) and the PCC2FOS plasmid construct containing human NOS3 full-length green fluorescent protein (GFP)-tagged gene including the promoter sequence and introns (code number NANOS3-GFP-001; SpectraGenetics) were used for in vitro transient transfection experiments. HEK-293 cells were grown in DMEM F-12 medium supplemented with 10% fetal bovine serum, 100 U/mL penicil-

**Table 1.** Calcium and Phosphate Homeostasis in 3- and 9-Month-Old Male WT and VDR$^{\Delta/\Delta}$ Mice Fed the Rescue Diet

| Variable | 3-Month-Old | | 9-Month-Old | |
| | WT | VDR$^{\Delta/\Delta}$ | WT | VDR$^{\Delta/\Delta}$ |
| --- | --- | --- | --- | --- |
| Serum calcium, mmol/L | 2.22 ± 0.10 | 2.09 ± 0.06 | 2.26 ± 0.20 | 2.17 ± 0.15 |
| Ionized blood Ca$^{2+}$, mmol/L | 1.29 ± 0.04 | 1.24 ± 0.10 | 1.31 ± 0.06 | 1.20 ± 0.10 |
| Serum phosphate, mmol/L | 3.17 ± 0.44 | 2.49 ± 0.39 | 3.43 ± 0.29 | 3.42 ± 0.48 |
| Serum 1,25(OH)$_2$D, pmol/L | 38.70 ± 18.20 | 373.00 ± 57.10[a] | 48.27 ± 15.70 | 558.44 ± 45.20[a] |
| Serum PTH, pg/mL | 31.20 ± 12.20 | 173.50 ± 48.80[a] | 15.30 ± 7.20 | 165.51 ± 39.20[a] |

All values are means ± SD of 7 to 10 animals in each group.

[a] $P < .05$ vs WT by $t$ test.

**Figure 1.** Mean arterial pressure and the RAAS are unchanged in VDR-deficient mice fed the rescue diet. A, Ratio of heart weight (HW) to body weight (BW) in WT and VDR$^{\Delta/\Delta}$ mice. B, Representative histological heart sections demonstrating cardiac hypertrophy in VDR$^{\Delta/\Delta}$ mice. Hematoxylin and eosin staining after perfusion fixation of 9-month-old mice. C, Mean arterial pressure (MAP) in the ascending aorta. D, Kidney renin mRNA levels were elevated in 9-month-old VDR$^{\Delta/\Delta}$ mice fed the normal diet (ND, left) but not in VDR$^{\Delta/\Delta}$ mice fed the rescue diet (RD, right) enriched in calcium, phosphate, and lactose. E and F, Serum (E) and urinary (F) aldosterone levels were elevated in 9-month-old VDR$^{\Delta/\Delta}$ mice fed the normal diet but not those fed the rescue diet as measured by ELISA. No differences between the groups were observed in renin mRNA or aldosterone levels at 3 months of age. G, Plasma renin activity (PRA) was similar in 3- and 9-month-old WT and VDR$^{\Delta/\Delta}$ mice fed the rescue diet. Values in A and C to G are means ± SEM of 4 to 8 mice per group. *, $P < .05$ comparing VDR$^{\Delta/\Delta}$ with WT mice fed the same diet.

lin, and 100 $\mu$g/mL streptomycin at 37°C in a 5% $CO_2$/95% air-humidified atmosphere. Twenty-four hours after seeding, cells at ~70% confluence were subjected to transient transfection using X-tremeGENE 9DNA transfection reagent (Roche) according to the manufacturer's protocol. The cells were cotransfected with 1 $\mu$g of each construct. Twenty-four hours after transfection, the cells were treated with $10^{-7}$ to $10^{-10}$ M 1$\alpha$,25-dihydroxyvitamin D$_3$ (Sigma-Aldrich) or vehicle. NOS3 expression was monitored by GFP expression quantification in triplicate at 24, 48, and 72 hours after stimulation, using a commercial assay system (BioVision) and a fluorescence microplate reader (EnSpire 2300 Multilabel reader; PerkinElmer).

### Statistical analyses

Statistics were computed using SPSS for Windows 17.0. The data were analyzed by a two-sided $t$ test (2 groups) or one-way analysis of variance (ANOVA) followed by Student-Newman-Keuls multiple comparison test (>2 groups). Values of $P < .05$ were considered significant. The data are presented as means ± SEM in the figures and as means ± SD in Table 1.
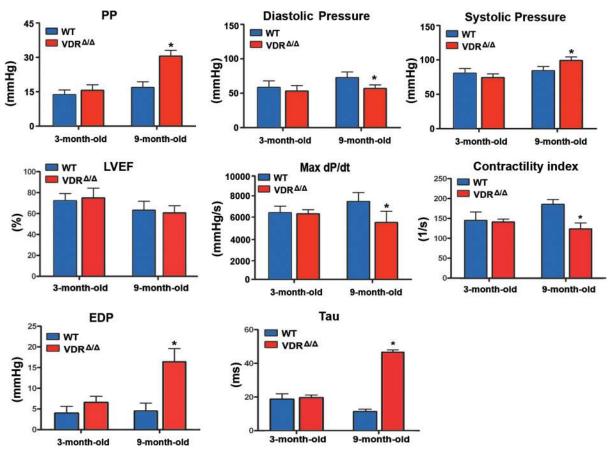
## Results

Although serum calcium, ionized blood calcium, and serum phosphorus were not significantly different in 3- and 9-month-old WT and VDR$^{\Delta/\Delta}$ mice fed the rescue diet, the rescue diet did not completely normalize serum PTH in VDR-deficient mice in this experiment (Table 1). However, compared with the severe secondary hyperparathyroidism present in VDR$^{\Delta/\Delta}$ mice fed the normal diet (mean ± SD, 1290 ± 418 and 2266 ± 806 pg/mL in 3- and 9-month-old VDR$^{\Delta/\Delta}$ mice, respectively), the increase in serum PTH observed in VDR$^{\Delta/\Delta}$ mice fed the rescue diet was moderate. In agreement with the known fact that feedback inhibition of renal 1$\alpha$-hydroxylase requires the liganded and functional VDR (22), circulating 1,25(OH)$_2$D was increased in VDR-deficient mice (Table 1).
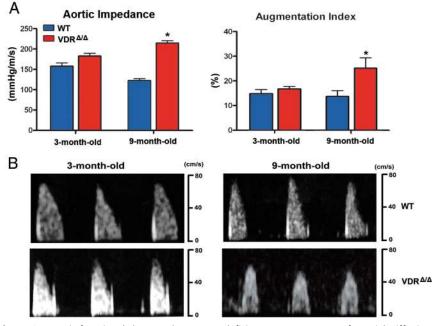
In accordance with earlier studies in global VDR knockout mice fed a normal diet (9), we found a clear increase in the heart to body weight ratio in 9-month-old male VDR$^{\Delta/\Delta}$ mice fed the rescue diet (Figure 1). However, there was only a nonsignificant trend toward a higher heart to body weight ratio in young adult (3 months old) male VDR$^{\Delta/\Delta}$ mice (Figure 1A). Higher LV muscle mass in 9-month-old VDR$^{\Delta/\Delta}$ mice was also evident in histological sections (Figure 1B). To our surprise, arterial catheterization revealed unchanged mean arterial pressure in 3- and 9-month-old VDR$^{\Delta/\Delta}$ mice fed the rescue diet (Figure 1C). In accordance with this finding, kidney renin mRNA levels as well as serum and urinary aldosterone and plasma renin activity were not different between WT and VDR$^{\Delta/\Delta}$ mice fed the rescue diet (Figure 1, D–G). Similarly, human patients with defective VDR function show unaltered plasma renin activity (23). However, we detected increased renin mRNA abundance and aldosterone levels in 9-month-old VDR$^{\Delta/\Delta}$ mice fed a normal diet, showing that the changes in RAAS in VDR mutant mice are driven by secondary hyperparathyroidism (Figure 1, D–F). These findings suggest that the increased

heart to body weight ratio in 9-month-old VDR$^{\Delta/\Delta}$ mice fed the rescue diet was not caused by increased mean arterial pressure due to an overactivated RAAS.

However, when we performed the arterial catheterization experiments, we made an unexpected and interesting discovery. Although mean arterial pressure was not changed, arterial pulse pressure was profoundly increased in 9-month-old, but not in young adult, VDR$^{\Delta/\Delta}$ mice compared with WT controls (Figure 2). The increased pulse pressure in older VDR$^{\Delta/\Delta}$ mice was the result of increased central systolic pressure and decreased diastolic pressure (Figure 2). Heart rate did not differ between WT and VDR mutant mice, independent of age (Supplemental Figure 1A published on The Endocrine Society's Journals Online web site at http://mend.endojournals.org.). We initially reasoned that the increase in pulse pressure could be due to a greater stroke volume or increased contractility of the myocardium in the absence of a functioning VDR. Therefore, we examined functional heart parameters.

VDR$^{\Delta/\Delta}$ mice were characterized by a normal ejection fraction (Figure 2) and normal fractional shortening (Supplemental Figure 1C) as determined by echocardiography

**Figure 2.** VDR deficiency alters vascular and cardiac parameters in aged mice. Aortic and cardiac pressure analysis by catheterization of the ascending aorta and left ventricle. Values are means ± SEM of 4 to 8 mice per group. *, $P < .05$ comparing 9-month-old VDR$^{\Delta/\Delta}$ with WT mice. PP, pulse pressure; LVEF, LV ejection fraction measured by echocardiography; Max dP/dt, the first derivative of the developed pressure; EDP, end-diastolic LV pressure; Tau, isovolumetric relaxation time.

**Figure 3.** Aortic functional changes due to VDR deficiency. A, Parameters of arterial stiffening are increased in 9-month-old VDR$^{\Delta/\Delta}$ mice. Ascending aortic impedance (left) was evaluated as the ratio of aortic pressure to luminal average blood velocity (n = 4–8 each). Augmentation index (right) was calculated as a ratio of the pressure at the augmentation point and the pulse pressure (n = 4–8 each). B, Representative Doppler echograms of the aortic flow velocities recorded in WT mice (top panels) and VDR$^{\Delta/\Delta}$ mice (bottom panels). Values are means ± SEM. *, $P < .05$ comparing 9-month-old VDR$^{\Delta/\Delta}$ with WT mice.

We therefore set out to investigate whether VDR signaling indeed affects aortic input impedance, an index of arterial stiffness. We simultaneously acquired pressure and velocity signals and calculated aortic input impedance as the ratio of the mean arterial pressure to luminal average blood velocity (14). In young mice, the aortic input impedance index was slightly, but not significantly higher in VDR$^{\Delta/\Delta}$ than in WT mice (Figure 3). However, in 9-month-old mice the aortic impedance index rose significantly from 122 ± 5 mm Hg/m/s in WT mice to 215 ± 6 mm Hg/m/s in VDR$^{\Delta/\Delta}$ mice (Figure 3A). In addition, pulse wave analysis of pressure traces recorded in the ascending aorta revealed a significant increase in the augmentation pressure and augmentation index in 9-month-old VDR$^{\Delta/\Delta}$ mice, whereas young VDR$^{\Delta/\Delta}$ mice had only slightly increased augmentation pressure and augmentation index (Figure 3B and data not shown). These findings demonstrate that long-term lack of VDR signaling increases aortic impedance and peripheral wave reflections.

Because the elastic properties of the aorta are a major determinant of the aortic impedance (25), we further analyzed the collagen and elastin content of the ascending aorta. We found a 1.9-fold higher collagen content and a 3.4-fold lower elastin content in 9-month-old VDR$^{\Delta/\Delta}$ mice than in WT mice (Figure 4). In young animals, we did not observe any differences in collagen and elastin content between WT and VDR$^{\Delta/\Delta}$ mice (Figure 4A). At the light microscopic level, there were no obvious morphological differences between the aortas of 9-month-old WT and VDR$^{\Delta/\Delta}$ mice (Figure 4B). However, scanning electron microscopy images visualized the striking decrease in elastin fibers in aortas from 9-month-old VDR$^{\Delta/\Delta}$ compared with WT mice (Figure 4C). The increased aortic collagen and reduced elastin content would explain the increased aortic impedance in 9-month-old VDR mutant mice. However, the fact that these changes were absent in 3-month-old VDR$^{\Delta/\Delta}$ mice suggests that the switch in the content of aortic structural proteins is probably reactive and does not represent the primary mechanism that increases aortic impedance and pulse wave reflections.

both at young and older ages. However, cardiac catheterization revealed deterioration of inotropic cardiac parameters including the maximum rate of LV pressure rise and contractility index in 9-month-old VDR$^{\Delta/\Delta}$ mice (Figure 2). Diastolic function was also affected as indicated by the rise in end-diastolic pressure and prolongation of isovolumetric relaxation time (Tau) (Figure 2). Cardiac function was unchanged in young adult VDR$^{\Delta/\Delta}$ mice (Figure 2). In addition, there were no signs of cardiac fibrosis (Supplemental Figure 1B) or lung congestion as evidenced by a normal lung to body weight ratio (Supplemental Figure 1D) in young and older VDR$^{\Delta/\Delta}$ mice. These findings indicate compensated systolic and diastolic dysfunction in 9-month-old VDR mutants and rule out increased contractility or stroke volume as a cause for the increased pulse pressure observed in these animals.
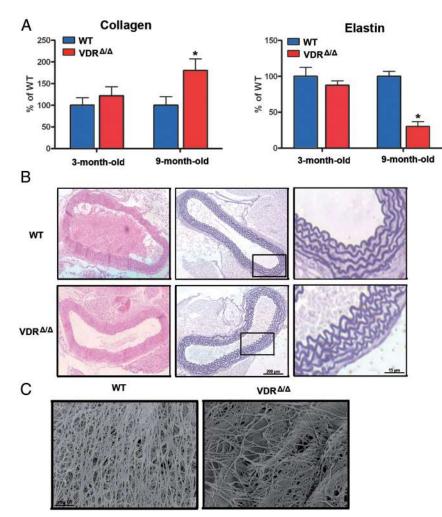
Notably, the pulse pressure elevation was associated with the development of the cardiac phenotype, as both were evident in older but not in young VDR$^{\Delta/\Delta}$ mice. Elevated pulse pressure may also reflect increased arterial stiffness. It is well known that increased arterial stiffness raises systolic pressure and decreases diastolic pressure, due to augmented peripheral wave reflections and their earlier arrival to the proximal aorta during the cardiac cycle (24). This fact led us to hypothesize that increased stiffening of the arterial system may underlie or at least contribute to the cardiac hypertrophy and dysfunction in VDR$^{\Delta/\Delta}$ mice.

Another important determinant of arterial stiffness is endothelial function, ie, the balance in endothelial secre-

**Figure 4.** Aortic structural changes in VDR-deficient mice. A, Changes in the collagen and elastin protein content in the thoracic aorta of VDR$^{\Delta/\Delta}$ mice. Bars are collagen/elastin content expressed as a percentage of that of WT mice at the respective age (n = 6–9 each). B, Representative histological thoracic aorta sections stained with hematoxylin and eosin (left) and elastic lamellae stained by resorcin-fuchsin (middle and right) in 9-month-old WT and VDR$^{\Delta/\Delta}$ mice. Right panels are higher magnification views of the insets depicted in middle panels. C, Scanning electron micrograph of elastin residues in the thoracic aorta of 9-month-old WT and VDR$^{\Delta/\Delta}$ mice. Values are means ± SEM. *, $P < .05$ comparing 9-month-old VDR$^{\Delta/\Delta}$ with WT mice.

duced nitrite/nitrate levels both in serum and urine (Figure 5).

NOS3 is the main source of vascular NO. To examine whether VDR signaling controls *NOS3* gene expression, we quantified *NOS3* mRNA abundance in aortas from VDR$^{\Delta/\Delta}$ and WT control mice. Both 3- and 9-month-old VDR$^{\Delta/\Delta}$ mice showed decreased aortic expression of *NOS3* (Figure 5B). Along similar lines, NOS3 protein expression was about 3-fold lower in aortas of 3- and 9-month-old VDR$^{\Delta/\Delta}$ mice, relative to that of WT controls (Figure 5C). Apart from reduced NOS3 levels, limited availability of L-arginine may underlie the decreased NO production in VDR$^{\Delta/\Delta}$ mice. Arginases compete with NOS for the substrate L-arginine and hydrolyze it to ornithine and urea. Their increased activity has been demonstrated in aged or diseased vessels where they contribute to endothelial dysfunction, smooth muscle cell proliferation, and vascular fibrosis (30–32). Aortic mRNA expression of arginase I tended to be nonsignificantly higher in 3- and 9-month-old VDR$^{\Delta/\Delta}$ mice, whereas aortic arginase II expression was significantly increased in 9-month-old VDR$^{\Delta/\Delta}$ mice relative to that in WT controls (Supplemental Figure 2A). Although not entirely consistent, these data suggest that VDR-dependent regulation of arginases might also be involved in the lower NO production in VDR$^{\Delta/\Delta}$ mice. Nevertheless, our finding that loss of VDR signaling impairs NO availability and aortic *NOS3* gene and protein expression in 3-month-old mice suggests that reduced endothelial NO production may represent the primary event in the development of cardiovascular disease in VDR-deficient mice.

We next investigated whether vitamin D can act directly on vessels to regulate NOS3 expression. VDR$^{\Delta/\Delta}$ mice carry a *lacZ* reporter gene cassette driven by the endogenous *VDR* gene promoter. Using parathyroid glands as a positive control, we found strong *lacZ* expression in the endothelial layer of the thoracic aorta as well as in the smooth muscle cells between elastic lamellas in VDR$^{\Delta/\Delta}$ mice (Figure 6). These findings suggest that VDR is expressed in endothelial and vascular smooth muscle
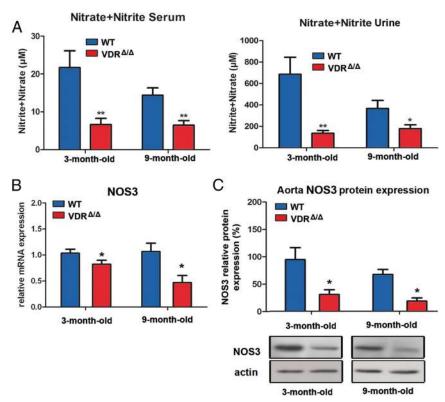
tion of vasodilating and vasoconstricting factors (26, 27). Several lines of evidence suggest that vitamin D may regulate endothelial function. In vitro, 1,25(OH)$_2$D$_3$ decreases endothelium-dependent contraction of aortic rings by reducing the increase in cytosolic free calcium concentration in endothelial cells, although the exact mechanism is not known (28). In clinically healthy subjects, serum 25(OH)D levels positively correlate with brachial flow–mediated dilation, a measure of endothelium-dependent dilation (29). Release of endothelial NO is considered a major determinant of endothelium-dependent vasodilation. To test whether ablation of VDR signaling affects NO bioavailability in vivo, we analyzed the levels of the NO metabolites nitrite and nitrate in biological fluids. Compared with their WT littermates, young and 9-month-old VDR$^{\Delta/\Delta}$ mice had 2- to 3-fold re-

**Figure 5.** VDR controls NO production and *NOS3* gene expression in vivo. A, NO production assessed by measuring nitrite and nitrate levels in ultrafiltrated serum (n = 4–8 each), and urine (n = 6 each). B, Reduced mRNA expression of NOS3 in the aorta of VDR$^{\Delta/\Delta}$ mice (n = 5–8 each). C, Reduced aortic protein expression of NOS3 in VDR$^{\Delta/\Delta}$ mice (n = 4–6 each). Values are means ± SEM. *, $P < .05$; **, $P < .01$ comparing VDR$^{\Delta/\Delta}$ with WT mice.

cells, which is in agreement with previous reports (33). To quantify the relative VDR expression in aortic endothelial and smooth muscle cells, we performed laser capture microdissection on cryosections from aortas of 9-month-old WT and VDR$^{\Delta/\Delta}$ mice. The relative abundance of VDR transcripts was about twice as high in smooth muscle cells as in endothelium in WT mice and negligible in VDR$^{\Delta/\Delta}$ mice, using primers amplifying the deleted exon 2, which codes for the DNA-binding domain of the VDR (Figure 6B). VDR$^{\Delta/\Delta}$ mice express a nonfunctional VDR lacking the DNA binding domain (12). As a control for the quality of the preparation, we also quantified *NOS3* mRNA in these samples. We found reduced *NOS3* mRNA expression in the endothelium of VDR$^{\Delta/\Delta}$ mice relative to that in WT mice, but very low levels in smooth muscle cells, thereby confirming that our results did not relate to contamination of endothelium by smooth muscle cells. Taken together, these results clearly demonstrate the presence of VDR in murine aortic endothelium.

To examine whether 1,25(OH)$_2$D$_3$ is a positive regulator of *NOS3* gene expression in gain-of-function experiments, we treated aortic rings from WT mice with 1,25(OH)$_2$D$_3$ in organ culture. Indeed, 10 nM 1,25(OH)$_2$D$_3$ induced an almost 4-fold up-regulation in aortic *NOS3* mRNA abun-
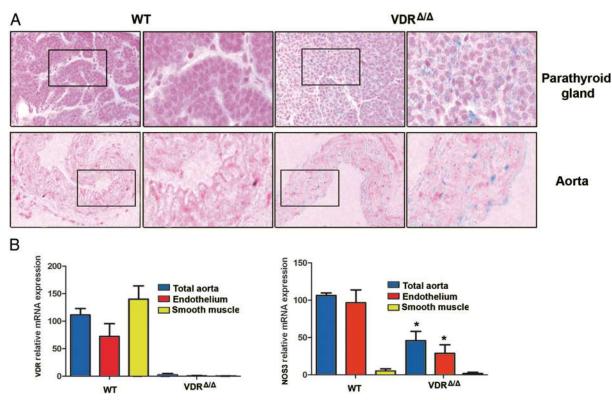
dance in vitro (Figure 7). Treatment of aortic rings with 1,25(OH)$_2$D$_3$ also decreased arginase I, but not arginase II, gene expression (Supplemental Figure 2B). Moreover, *NOS3* gene expression was stimulated by 100 nM 25(OH)D$_3$ (Figure 7A), suggesting that 25(OH)D$_3$ can be locally activated in aortic organ cultures. In agreement with this finding, bovine aortic endothelial cells have been shown to express 1α-hydroxylase (33). The stimulation of *NOS3* expression by both 1,25(OH)$_2$D$_3$ and 25(OH)D$_3$ was abrogated in aortic rings from VDR$^{\Delta/\Delta}$ mice (Figure 7A), indicating that this effect is dependent on intact VDR signaling.

Finally, we examined whether 1,25(OH)$_2$D$_3$ is a direct transcriptional regulator of the *NOS3* gene. Genomatix software predicted 3 putative VDR binding sites at −128, −451, and −923 and at −185, −254, and −736 bp upstream of the transcriptional start site within the human and murine *NOS3* promoter, respectively, but only 1 putative vitamin D response element in the arginase I pro-

moter at −518 bp upstream of the transcriptional start site and none in the arginase II promoter. To analyze the direct effects of vitamin D signaling on *NOS3* transcriptional activity, we performed transient double transfection of HEK cells with human VDR plasmids and the full-length human *NOS3* gene fused to a GFP reporter gene. Stimulation of transfected cells with 0.1 to 100 nM 1,25(OH)$_2$D$_3$ dose dependently up-regulated expression of the NOS3-GFP fusion protein within 24 hours (Figure 7B) and at later time points (Supplemental Figure 3, A and B). 1,25(OH)$_2$D$_3$ did not stimulate expression of the fusion protein in the absence of cotransfected human VDR (Figure 7B). These data demonstrate that 1,25(OH)$_2$D$_3$ is a direct transcriptional regulator of *hNOS3*.

## Discussion

In this study we aimed to decipher the mechanisms by which 1,25(OH)$_2$D$_3$ may regulate systemic vascular tone and cardiac function. Here we provide evidence that loss of VDR signaling increases arterial stiffness and results in systolic and diastolic cardiac impairment, independent of activation of the RAAS. We propose a VDR-driven mech-

**Figure 6.** VDR and NOS3 expression in aortic endothelial and smooth muscle cells. A, LacZ reporter gene expression visualized by X-Gal staining to detect localization of the VDR. Intense staining is present in the endothelial and medial layer of the thoracic aorta (blue) in the VDR$^{\Delta/\Delta}$ mouse, whereas staining is completely absent in the WT mouse. The parathyroid gland was used as a positive control for VDR expression. Right panels are higher magnification views of the insets depicted in the left panels. B, mRNA expression of VDR and NOS3 in the endothelial and smooth muscle layer harvested by laser capture microdissection from cryosections of the thoracic aorta from 9-month-old WT and VDR$^{\Delta/\Delta}$ mice and normalized to the total aorta preparation. Values are means ± SEM. *, $P < .05$ comparing VDR$^{\Delta/\Delta}$ with WT mice (4–5 samples per group).

anism that regulates NO production by enhancing the transcription of its main endothelial synthesizing enzyme, NOS3. This model is shown in Figure 8. In addition, 1,25(OH)$_2$D$_3$ may increase NO production in endothelial cells via rapid nongenomic activation of NOS3 by a VDR-dependent phosphorylation cascade (34). The role of vascular smooth muscle cells in mediating the vascular effects of vitamin D is currently unclear. Because 1,25(OH)$_2$D$_3$ is known to regulate a variety of genes in vascular smooth muscle cells (35), it is conceivable that VDR deficiency may also alter the response of vascular smooth muscle cells to NO, or, in more general terms, 1,25(OH)$_2$D$_3$ might affect the cross-talk between endothelium and smooth muscle cells in blood vessels. However, firm evidence for such an additional function of 1,25(OH)$_2$D$_3$ is currently lacking.

In our explanatory model, reduced NO production already present in young VDR$^{\Delta/\Delta}$ mice results over time in arterial stiffening and increased pulse pressure, leading to altered collagen and elastin content in the aorta by long-term increases in mechanical strain and to cardiac functional impairment by chronically increased afterload at older ages. If our hypothesis that the vascular phenotype of VDR$^{\Delta/\Delta}$ mice is mainly driven by reduced NO produc-

tion is correct, VDR$^{\Delta/\Delta}$ mice should partially recapitulate the phenotype of NOS3 knockout mice. Indeed, global NOS3 knockout mice, an ultimate model of endothelial dysfunction, develop hypertension and compensated concentric LV hypertrophy due to increased afterload (36, 37), similar to VDR$^{\Delta/\Delta}$ mice. In addition, it was recently shown that aortas of NOS3 knockout mice are stiffer than those of WT controls due to increased matrix cross-linking by augmented transglutaminase activity (38). We did not examine matrix cross-linking in our study. Nevertheless, our findings of increased arterial stiffness and structural aortic changes developing over months in VDR$^{\Delta/\Delta}$ mice characterized by mild NO deficiency is in full agreement with the observation of arterial stiffening and increased pulse wave velocity in NOS3 knockout mice (38). A potential limitation of our study is that the rescue diet did not completely normalize serum PTH levels in VDR$^{\Delta/\Delta}$ mice. Therefore, increased circulating PTH may have contributed to the observed phenotype. However, it has been reported that PTH stimulates NOS3 expression and activity in human umbilical cord vein endothelial cells (39). Therefore, it is not likely that the down-regulation of NOS3 in VDR$^{\Delta/\Delta}$ mice can be explained by
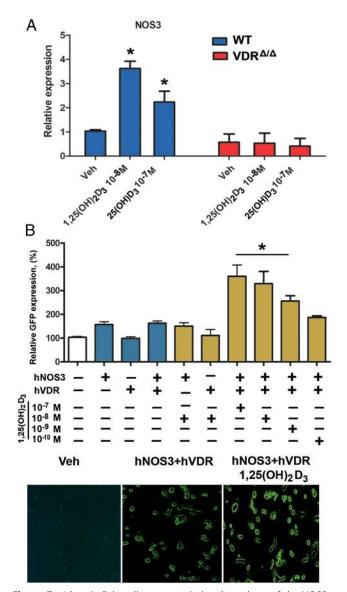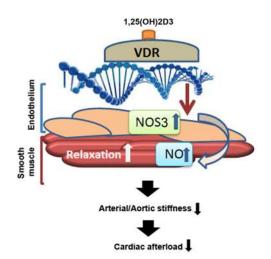
**Figure 7.** Vitamin D is a direct transcriptional regulator of the NOS3 gene. A, In vitro exposure to $1,25(OH)_2D_3$ and $25(OH)D_3$ stimulated expression of *NOS3* mRNA in the aorta. Rings of the thoracic aorta isolated from 3-month-old WT and VDR$^{\Delta/\Delta}$ mice were incubated with $10^{-8}$ M $1,25(OH)_2D_3$, $10^{-7}$ M $25(OH)D_3$, or vehicle (Veh, ethanol) for 24 hours in organ culture (n = 3 each). B, $1,25(OH)_2D_3$ increases *NOS3* gene transcription in HEK-293 cells transiently transfected with the pCMV6 plasmid construct containing human VDR (hVDR) and the PCC2FOS plasmid construct containing the full-length human NOS3 GFP-tagged gene, including the promoter region (hNOS3). GFP expression (4–6 samples per group) was determined 24 hours after stimulation with $10^{-10}$, $10^{-9}$, $10^{-8}$, or $10^{-7}$ M $1,25(OH)_2D_3$ or vehicle (ethanol). Values are means ± SEM. *, $P < .05$ comparing $1,25(OH)_2D_3$ vs vehicle (in A) or $1,25(OH)_2D_3$ vs vehicle (double-transfected HEK-293 cells) and vs NOS3 single-transfected HEK-293 cells (vehicle and $1,25(OH)_2D_3$ treatment) (in B).

the mild secondary hyperparathyroidism observed in these mice in our study.

It has been shown that cardiomyocyte-specific VDR ablation also induces heart hypertrophy by unleashing the prohypertrophic calcineurin/nuclear factor of the acti-



**Figure 8.** VDR-driven mechanism regulating endothelial NO production by stimulation of NOS3 transcription. After binding to its ligand $1,25(OH)_2D_3$, the activated VDR stimulates *NOS3* transcription, resulting in increased production of NO, which in turn causes vascular smooth muscle cell relaxation, thereby reducing arterial stiffness and cardiac afterload.

vated T-cell signaling pathway (10). Therefore, the cardiac phenotype observed in VDR$^{\Delta/\Delta}$ mice is probably a combination of loss of protective VDR signaling within cardiomyocytes and increased afterload by endothelial dysfunction and increased arterial stiffness. Because NOS3 is also expressed in cardiomyocytes, our findings may shed some new light on the recent study by Chen et al (10) in cardiomyocyte-specific VDR-ablated mice. In fact, cardiomyocytes account for approximately 20% total cardiac NOS3 protein (40). Based on our data, is it conceivable that $1,25(OH)_2D_3$ may also regulate NOS3 in cardiomyocytes and that this mechanism may contribute to the heart phenotype seen in VDR-ablated mice. It is well known that NOS3 in cardiomyocytes is cardioprotective. Cardiomyocyte-specific overexpression of NOS3 improves LV performance and reduces compensatory hypertrophy after myocardial infarction (41). Moreover, NOS3 modulates the β-adrenergic and muscarinic response in isolated cardiomyocytes (42). The latter observation points to the beneficial effect of NOS3 in conditions where excessive adrenergic input is likely to damage the myocardium, such as the failing heart. Therefore, it is obvious that the role of the VDR in the regulation of NOS3 expression in cardiomyocytes needs further investigation.

We believe that the current study adds to our understanding of how VDR signaling regulates cardiovascular function. Furthermore, our data may provide a mechanistic explanation for hitherto unexplained epidemiological data in humans and may have important clinical implications for the treatment of cardiovascular diseases. Clinical trials examining the cardiovascular effects of vitamin D

supplementation have been inclusive thus far. In accordance with our findings, Dong et al (43) reported a decrease in pulse wave velocity in response to high-dose vitamin D supplementation in a randomized, controlled clinical trial in black adolescents. Similarly, $1,25(OH)_2D_3$ improved endothelial function in spontaneously hypertensive rats in vivo and in renal arteries of hypertensive patients in vitro (44). However, other clinical trials reported negative results for vitamin D supplementation on aortic stiffness and endothelial dysfunction in elderly patients (45, 46). In part, the discrepant clinical findings may be explained by the requirement of local VDR activation in blood vessels to elicit biological effects. Therefore, only the local intracellular concentration of the VDR agonist $1,25(OH)_2D_3$, but not that of vitamin D and $25(OH)D$ in serum, may be directly associated with beneficial treatment effects. In this context, local activation of $25(OH)D_3$ by $1\alpha$-hydroxylase in endothelial cells may be an important modulator of the biological effects of circulating $25(OH)D_3$ on blood vessels. Based on our data, it may be worthwhile to explore the possibility of developing endothelium-selective VDR agonists for the improvement of endothelial function and the reduction of arterial stiffness in patients.

## Acknowledgments

## References

1. **Scragg R, Sowers M, Bell C.** Serum 25-hydroxyvitamin D, ethnicity, and blood pressure in the Third National Health and Nutrition Examination Survey. *Am J Hypertens*. 2007;20:713–719.
2. **Judd SE, Nanes MS, Ziegler TR, Wilson PW, Tangpricha V.** Optimal vitamin D status attenuates the age-associated increase in systolic blood pressure in white Americans: results from the third National Health and Nutrition Examination Survey. *Am J Clin Nutr*. 2008;87:136–141.
3. **Pittas AG, Chung M, Trikalinos T, et al.** Systematic review: Vitamin D and cardiometabolic outcomes. *Ann Intern Med*. 2010;152:307–314.
4. **Al Mheid I, Patel R, Murrow J, et al.** Vitamin D status is associated with arterial stiffness and vascular dysfunction in healthy humans. *J Am Coll Cardiol*. 2011;58:186–192.
5. **Chitalia N, Recio-Mayoral A, Kaski JC, Banerjee D.** Vitamin D deficiency and endothelial dysfunction in non-dialysis chronic kidney disease patients. *Atherosclerosis*. 2012;220:265–268.
6. **Yiu YF, Chan YH, Yiu KH, et al.** Vitamin D deficiency is associated with depletion of circulating endothelial progenitor cells and endothelial dysfunction in patients with type 2 diabetes. *J Clin Endocrinol Metab*. 2011;96:E830–E835.
7. **London GM, Guérin AP, Verbeke FH, et al.** Mineral metabolism and arterial functions in end-stage renal disease: potential role of 25-hydroxyvitamin D deficiency. *J Am Soc Nephrol*. 2007;18:613–620.
8. **Bodnar LM, Catov JM, Simhan HN, Holick MF, Powers RW, Roberts JM.** Maternal vitamin D deficiency increases the risk of preeclampsia. *J Clin Endocrinol Metab*. 2007;92:3517–3522.
9. **Li YC, Kong J, Wei M, Chen ZF, Liu SQ, Cao LP.** 1,25-Dihydroxyvitamin $D_3$ is a negative endocrine regulator of the renin-angiotensin system. *J Clin Invest*. 2002;110:229–238.
10. **Chen S, Law CS, Grigsby CL, et al.** Cardiomyocyte-specific deletion of the vitamin D receptor gene results in cardiac hypertrophy. *Circulation*. 2011;124:1838–1847.
11. **Elliott P, McKenna WJ.** Hypertrophic cardiomyopathy. *Lancet*. 2004;363:1881–1891.
12. **Erben RG, Soegiarto DW, Weber K, et al.** Deletion of deoxyribonucleic acid binding domain of the vitamin D receptor abrogates genomic and nongenomic functions of vitamin D. *Mol Endocrinol*. 2002;16:1524–1537.
13. **Li YC, Amling M, Pirro AE, et al.** Normalization of mineral ion homeostasis by dietary means prevents hyperparathyroidism, rickets, and osteomalacia, but not alopecia in vitamin D receptor-ablated mice. *Endocrinology*. 1998;139:4391–4396.
14. **Reddy AK, Li YH, Pham TT, et al.** Measurement of aortic input impedance in mice: effects of age on aortic stiffness. *Am J Physiol Heart Circ Physiol*. 2003;285:H1464–H1470.
15. **Vaitkevicius PV, Fleg JL, Engel JH, et al.** Effects of age and aerobic capacity on arterial stiffness in healthy adults. *Circulation*. 1993;88:1456–1462.
16. **Kelly R, Hayward C, Avolio A, O'Rourke M.** Noninvasive determination of age-related changes in the human arterial pulse. *Circulation*. 1989;80:1652–1659.
17. **Wolinsky H.** Response of the rat aortic wall to hypertension: importance of comparing absolute amounts of wall components. *Atherosclerosis*. 1970;11:251–255.
18. **Woessner JF Jr.** The determination of hydroxyproline in tissue and protein samples containing small proportions of this imino acid. *Arch Biochem Biophys*. 1961;93:440–447.
19. **Keeley FW, Morin JD, Vesely S.** Characterization of collagen from normal human sclera. *Exp Eye Res*. 1984;39:533–542.
20. **Pfaffl MW.** A new mathematical model for relative quantification in real-time RT-PCR. *Nucleic Acids Res*. 2001;29:e45.
21. **Gossler A, Zachgo J.** Gene and enhancer trap screens in ES cell chimeras. In: Joyner CJ, ed. *Gene Targeting: A Practical Approach*. New York, NY: Oxford University Press; 1993:181–227.
22. **Takeyama K, Kitanaka S, Sato T, Kobori M, Yanagisawa J, Kato S.** 25-Hydroxyvitamin $D_3$ $1\alpha$-hydroxylase and vitamin D synthesis. *Science*. 1997;277:1827–1830.
23. **Tiosano D, Schwartz Y, Braver Y, et al.** The renin-angiotensin system, blood pressure, and heart structure in patients with hereditary vitamin D-resistance rickets (HVDRR). *J Bone Miner Res*. 2011;26:2252–2260.

24. **O'Rourke MF, Staessen JA, Vlachopoulos C, Duprez D, Plante GE.** Clinical applications of arterial stiffness; definitions and reference values. *Am J Hypertens*. 2002;15:426–444.

25. **Safar ME, Levy BI, Struijker-Boudier H.** Current perspectives on arterial stiffness and pulse pressure in hypertension and cardiovascular diseases. *Circulation*. 2003;107:2864–2869.

26. **McEniery CM, Wallace S, Mackenzie IS, et al.** Endothelial function is associated with pulse pressure, pulse wave velocity, and augmentation index in healthy humans. *Hypertension*. 2006;48:602–608.

27. **Vanhoutte PM, Shimokawa H, Tang EH, Feletou M.** Endothelial dysfunction and vascular disease. *Acta Physiol (Oxf)*. 2009;196:193–222.

28. **Wong MS, Delansorne R, Man RY, Vanhoutte PM.** Vitamin D derivatives acutely reduce endothelium-dependent contractions in the aorta of the spontaneously hypertensive rat. *Am J Physiol Heart Circ Physiol*. 2008;295:H289–H296.

29. **Jablonski KL, Chonchol M, Pierce GL, Walker AE, Seals DR.** 25-Hydroxyvitamin D deficiency is associated with inflammation-linked vascular endothelial dysfunction in middle-aged and older adults. *Hypertension*. 2011;57:63–69.

30. **Berkowitz DE, White R, Li D, et al.** Arginase reciprocally regulates nitric oxide synthase activity and contributes to endothelial dysfunction in aging blood vessels. *Circulation*. 2003;108:2000–2006.

31. **Zhang C, Hein TW, Wang W, et al.** Upregulation of vascular arginase in hypertension decreases nitric oxide-mediated dilation of coronary arterioles. *Hypertension*. 2004;44:935–943.

32. **Romero MJ, Iddings JA, Platt DH, et al.** Diabetes-induced vascular dysfunction involves arginase I. *Am J Physiol Heart Circ Physiol*. 2012;302:H159–H166.

33. **Merke J, Milde P, Lewicka S, et al.** Identification and regulation of 1,25-dihydroxyvitamin $D_3$ receptor activity and biosynthesis of 1,25-dihydroxyvitamin $D_3$. Studies in cultured bovine aortic endothelial cells and human dermal capillaries. *J Clin Invest*. 1989;83:1903–1915.

34. **Molinari C, Uberti F, Grossini E, et al.** 1α,25-dihydroxycholecalciferol induces nitric oxide production in cultured endothelial cells. *Cell Physiol Biochem*. 2011;27:661–668.

35. **Wu-Wong JR, Nakane M, Ma J, Ruan X, Kroeger PE.** Elevated phosphorus modulates vitamin D receptor-mediated gene expression in human vascular smooth muscle cells. *Am J Physiol Renal Physiol*. 2007;293:F1592–F1604.

36. **Yang XP, Liu YH, Shesely EG, Bulagannawar M, Liu F, Carretero OA.** Endothelial nitric oxide gene knockout mice: cardiac phenotypes and the effect of angiotensin-converting enzyme inhibitor on myocardial ischemia/reperfusion injury. *Hypertension*. 1999;34:24–30.

37. **Shesely EG, Maeda N, Kim HS, et al.** Elevated blood pressures in mice lacking endothelial nitric oxide synthase. *Proc Natl Acad Sci USA*. 1996;93:13176–13181.

38. **Jung SM, Jandu S, Steppan J, et al.** Increased tissue transglutaminase activity contributes to central vascular stiffness in eNOS knockout mice. *Am J Physiol Heart Circ Physiol*. 2013;305:H803–H810.

39. **Rashid G, Bernheim J, Green J, Benchetrit S.** Parathyroid hormone stimulates the endothelial nitric oxide synthase through protein kinase A and C pathways. *Nephrol Dial Transplant*. 2007;22:2831–2837.

40. **Gödecke A, Heinicke T, Kamkin A, et al.** Inotropic response to β-adrenergic receptor stimulation and anti-adrenergic effect of ACh in endothelial NO synthase-deficient mouse hearts. *J Physiol*. 2001;532:195–204.

41. **Janssens S, Pokreisz P, Schoonjans L, et al.** Cardiomyocyte-specific overexpression of nitric oxide synthase 3 improves left ventricular performance and reduces compensatory hypertrophy after myocardial infarction. *Circ Res*. 2004;94:1256–1262.

42. **Massion PB, Dessy C, Desjardins F, et al.** Cardiomyocyte-restricted overexpression of endothelial nitric oxide synthase (NOS3) attenuates β-adrenergic stimulation and reinforces vagal inhibition of cardiac contraction. *Circulation*. 2004;110:2666–2672.

43. **Dong Y, Stallmann-Jorgensen IS, Pollock NK, et al.** A 16-week randomized clinical trial of 2000 international units daily vitamin $D_3$ supplementation in black youth: 25-hydroxyvitamin D, adiposity, and arterial stiffness. *J Clin Endocrinol Metab*. 2010;95:4584–4591.

44. **Dong J, Wong SL, Lau CW, et al.** Calcitriol restores renovascular function in estrogen-deficient rats through downregulation of cyclooxygenase-2 and the thromboxane-prostanoid receptor. *Kidney Int*. 2013;84:54–63.

45. **Gepner AD, Ramamurthy R, Krueger DC, Korcarz CE, Binkley N, Stein JH.** A prospective randomized controlled trial of the effects of vitamin D supplementation on cardiovascular disease risk. *PLoS One*. 2012;7:e36617.

46. **Stricker H, Tosi Bianda F, Guidicelli-Nicolosi S, Limoni C, Colucci G.** Effect of a single, oral, high-dose vitamin D supplementation on endothelial function in patients with peripheral arterial disease: a randomised controlled pilot study. *Eur J Vasc Endovasc Surg*. 2012;44:307–312.